

Allosteric inhibitors of Bcr-abl–dependent cell proliferation

Francisco J Adrián¹, Qiang Ding¹, Taebo Sim¹, Anastasia Velentza¹, Christine Sloan¹, Yi Liu¹, Guobao Zhang¹, Wooyoung Hur¹, Sheng Ding², Paul Manley³, Jürgen Mestan³, Dorian Fabbro³ & Nathanael S Gray¹

Chronic myelogenous leukemia (CML) is a myeloproliferative disorder characterized at the molecular level by the expression of Bcr-abl, a 210-kDa fusion protein with deregulated tyrosine kinase activity. Encouraged by the clinical validation of Bcr-abl as the target for the treatment of CML by imatinib, we sought to identify pharmacological agents that could target this kinase by a distinct mechanism. We report the discovery of a new class of Bcr-abl inhibitors using an unbiased differential cytotoxicity screen of a combinatorial kinase-directed heterocycle library. Compounds in this class (exemplified by GNF-2) show exclusive antiproliferative activity toward Bcr-abl–transformed cells, with potencies similar to imatinib, while showing no inhibition of the kinase activity of full-length or catalytic domain of c-abl. We propose that this new class of compounds inhibits Bcr-abl kinase activity through an allosteric non-ATP competitive mechanism.

The validation of Bcr-abl as a therapeutic target for the treatment of CML has been established with the clinical success of imatinib (STI571, Gleevec; Novartis Pharma). Imatinib is a phenylaminopyrimidine that inhibits the activity of Bcr-abl by binding to its ATP site and an adjacent allosteric site to effectively lock the kinase in an inactive conformation¹, thereby preventing transfer of phosphate from ATP to target proteins. Although treatment with imatinib during the chronic phase of CML usually results in a durable response, treatment during the accelerated or blast phase typically fails owing to the emergence of resistance mutations in the *BCR-ABL* gene^{2–4}. This has prompted the development of more potent Bcr-abl inhibitors such as AMN107 (ref. 5) and BMS-354825 (ref. 6).

Bcr-abl is a fusion protein with constitutive tyrosine kinase activity resulting from the combination of the *ABL1* (Abelson tyrosine kinase, c-abl) gene with the breakpoint cluster region gene (*BCR*). The c-abl kinase has a protein domain organization similar to that of Src kinases, with Src homology domains SH3 and SH2 followed by the catalytic domain (SH1 or KD)⁷. Despite the similarities to Src, the precise mechanism of its regulation was until recently unknown. Unlike with Src, which uses an intramolecular interaction between its SH2 domain and a C-terminal phosphotyrosine, structural studies of c-abl have shown an interaction between an N-terminal myristoyl group and a hydrophobic cleft located near the C terminus⁸. This intramolecular interaction may provide a mechanism for autoinhibition that would be disrupted in the Bcr-abl fusion protein.

Three general mechanisms for pharmacological inhibition of kinase activity have been identified: (i) direct competition with ATP in the ATP binding site (for example, the epidermal growth factor receptor

inhibitor gefitinib⁹, the cyclin-dependent kinase inhibitor roscovitine¹⁰); (ii) engagement of an adjacent allosteric binding site usually accessible when the activation loop and/or the α -C helix is folded away from the binding site, which results in kinase inactivation (for example, the Bcr-abl, platelet-derived growth factor receptor (PDGFR) and c-kit inhibitor imatinib¹¹, the p38 inhibitor BIRB 796 (ref. 12), the Raf inhibitor BAY43-9006 (refs. 13,14), the MAP kinase kinase inhibitor PD184352 (ref. 15)); and (iii) binding at sites remote from the ATP site that affect kinase activity (for example, Akt-I-1, a pleckstrin-homology-domain–dependent Akt (protein kinase B) inhibitor¹⁶, the glucokinase activator Ro-28-1675 (ref. 17)). To uncover new inhibitors of cellular Bcr-abl kinase, we performed a differential cytotoxicity screen in a 384-well format of approximately 50,000 combinatorially derived heterocycles¹⁸.

Here we report the discovery of a new class of Bcr-abl inhibitors that possess excellent selectivity toward Bcr-abl–transformed cells and maintain potency against clinically relevant imatinib-resistant Bcr-abl mutants. We propose that this class of compounds exert their activity through a newly described allosteric mechanism, potentially involving binding to the myristoyl pocket.

RESULTS

To identify compounds that could selectively inhibit the proliferation of Bcr-abl–dependent cell lines, we established a differential cytotoxicity screen that could be performed in a 384-well format. Such a cellular screen should provide an unbiased method to identify compounds that target any protein essential to Bcr-abl transformation.

¹Biological Chemistry Department, Genomics Institute of the Novartis Research Foundation, 10675 John Jay Hopkins Drive, San Diego, California 92121, USA.

²Department of Chemistry and the Skaggs Institute for Chemical Biology, The Scripps Research Institute, 10550 North Torrey Pines Road, La Jolla, California 92037, USA. ³Oncology Research, Novartis Institutes for Biomedical Research, CH-4002 Basel, Switzerland. Correspondence should be addressed to N.S.G. (ngray@gnf.org).

Received 9 August; accepted 2 December 2005; published online 15 January 2006; doi:10.1038/nchembio760

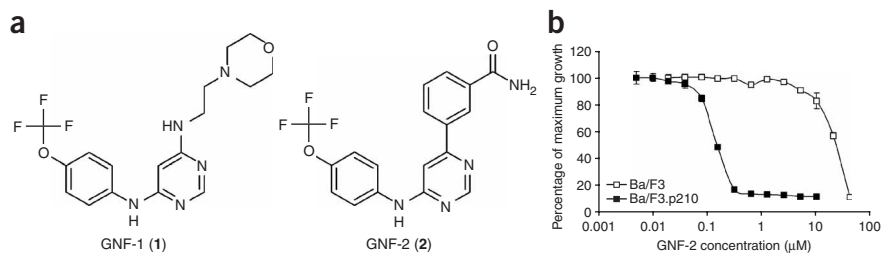


Figure 1 Cell proliferation. **(a)** Chemical structures of GNF-1 (**1**). **(b)** Ba/F3 and Ba/F3.p210 cells were incubated in the presence of increasing GNF-2 concentrations (0.02–40 μM and 0.005–10 μM , respectively) for 48 h. Cell viability at 48 h was measured by MTT uptake. Each point is the mean of duplicate experiments and indicates the percentage of cell growth in the absence of compound.

Lead compound identification and optimization

Several combinatorial compound libraries containing a total of approximately 50,000 compounds representing 30 different heterocyclic scaffolds¹⁸ were screened for their ability to inhibit the proliferation of 32D.p210 cells using a fluorescence-based proliferation assay, as described in the **Supplementary Methods** online. Compounds that inhibited proliferation by 80% at a concentration of 1 μM , as compared with the proliferation of the DMSO-treated cells, were tested for nonspecific cytotoxicity against nontransformed 32D cells. Compounds that resulted in a differential cytotoxicity of greater than ten-fold were then tested for their ability to inhibit recombinant abl kinase domain activity and cellular Bcr-abl autophosphorylation. After discarding many compounds that were well characterized as targeting the ATP binding site, such as phenylaminopyrimidines, 2,4-diaminopyrimidines, purines and pyrimidopyridinones, one compound of the 4,6-pyrimidine class, GNF-1 (**1**) (**Fig. 1a**), stood out in that it showed excellent differential cytotoxic activity, with a half-maximal inhibitory concentration (IC_{50}) of 400 nM for 32D.p210 Bcr-abl-expressing cells and an IC_{50} greater than 40 μM for 32D Bcr-abl-negative cells, without affecting recombinant abl kinase activity.

Subsequent medicinal chemistry optimization efforts, focused on improving antiproliferative activity against Bcr-abl-expressing cells, led to the synthesis of a series of more than 350 compounds showing clear cellular structure-activity relationships (Q.D., PCT Int. Appl. WO 2004089286. 2004). For example, there was a strict requirement for the 4-trifluoromethoxyaniline at the pyrimidine 4 position, a free aniline 4-NH, and a tolerance for a variety of substitutions at the pyrimidine C6 including cycloalkyl and aryl substituents, especially those with a *meta*-substituted H bond-accepting functionality (amide, sulfonamide, aniline). GNF-2 (**2**; **Fig. 1a**) is an example of a more potent cellular proliferation inhibitor in this compound series. The differential antiproliferative activity of this compound against Ba/F3 and Ba/F3.p210 cells is shown in **Fig. 1b**. GNF-2 specifically inhibited the proliferation of the Bcr-abl-expressing cells with an IC_{50} of 138 nM and did not show any cytotoxic effects on the nontransformed cells at concentrations of up to 10 μM . The Bcr-abl inhibitor imatinib, used as a positive control for inhibition, blocked the proliferation of these cell lines with IC_{50} values of 190 nM (Ba/F3.p210) and 20 μM (Ba/F3) (**Supplementary Table 1** online).

GNF-2 selectively inhibits Bcr-abl-dependent cell proliferation

To explore the specificity of GNF-2 for cells transformed by Bcr-abl, dose-response growth curves were generated in both Bcr-abl-positive (K562 and SUP-B15) and negative (HL60 and Jurkat) leukemic cells. Incubation with GNF-2 caused a dose-dependent growth inhibition of

the Bcr-abl-positive cell lines with IC_{50} values of 273 nM (K562) and 268 nM (SUP-B15). HL-60 and Jurkat cells were unaffected by this compound at concentrations below 10 μM (**Supplementary Table 1**).

We further investigated the cellular activity profile of GNF-2 against a panel of Ba/F3 cells transformed with other oncogenic kinases including Flt3-ITD, Tel-PDGFR β , TPR-MET and Tel-JAK1. The viability of these cell lines was not reduced after 48 h by treatment with concentrations of GNF-2 up to 10 μM (**Supplementary Table 1**). GNF-2 at concentrations of up to 10 μM did not inhibit the proliferation of Mo7e cells stimulated with either stem cell factor (c-kit-dependent

proliferation) or granulocyte-macrophage colony stimulating factor and a variety of lymphoma cell lines (RL-7, K422 and DoHH2). These results demonstrated that GNF-2 has antiproliferative activity solely against Bcr-abl-dependent cell lines.

GNF-2 inhibits E255V and Y253H mutant Bcr-abl cell growth

Diverse mutations within the BCR-ABL gene can lead to imatinib resistance in individuals with leukemia. Mutations at positions Thr315 and Glu255 account for up to 30% of mutations detected at the time of relapse¹⁹ and are resistant to inhibition by imatinib at clinically achievable doses. Compounds of the 4,6-disubstituted pyrimidine class proved to be efficient cell growth inhibitors of Ba/F3 cells expressing Bcr-abl with the mutations E255V or Y253H within the P loop. GNF-2 inhibited the growth of Ba/F3.p210^{E255V} and Ba/F3.p185^{Y253H} cells with IC_{50} values of 268 and 194 nM respectively, whereas 50% growth inhibition was not reached with 10 μM imatinib. Cells bearing the mutations M351T adjacent to the activation loop, or H396P within the activation loop, were less sensitive to GNF-2 (IC_{50} values of 752 and 3,269 nM, respectively). In contrast, GNF-2 did not affect the viability of Ba/F3 cells expressing Bcr-abl mutated at sites that directly contact imatinib (Thr315 and Phe317) or at positions Gly250 and Gln252 within the P loop at concentrations up to 5–10 μM (**Fig. 2a**).

GNF-2 induces apoptosis of Bcr-abl-transformed cells

Leukemic transformation mediated by Bcr-abl is known to inhibit apoptosis. To determine whether GNF-2 would induce apoptosis of the Bcr-abl-expressing cells, Ba/F3 and Ba/F3.p210 (wild type and E255V mutant) cells were cultured in the presence of different concentrations of GNF-2 for 48 h. Flow cytometric analysis of DNA content (**Fig. 2b**) showed an increased number of Ba/F3.p210 cells undergoing apoptosis when treated with GNF-2 concentrations as low as 1 μM for 48 h. Likewise, when Ba/F3.p210^{E255V} cells were cultured in the presence of 1 μM or higher concentration of GNF-2, they underwent apoptotic death after 48 h incubation. The viability of parental Ba/F3 cells was unaffected by GNF-2 concentrations below 10 μM .

IL-3 prevents antiproliferative and apoptotic effect of GNF-2

It has been described previously that interleukin 3 (IL-3) could reverse the antiproliferative and apoptotic activity of imatinib on Bcr-abl-transformed cells^{20–22}. To determine whether IL-3 could rescue Ba/F3.p210 and Ba/F3.p210^{E255V} cells from GNF-2-induced apoptotic death, we performed DNA staining-flow cytometric analysis after incubating the cells with 1 μM GNF-2 in the presence of IL-3. When 10 U ml⁻¹ IL-3 was added to the media, the apoptotic effect of GNF-2

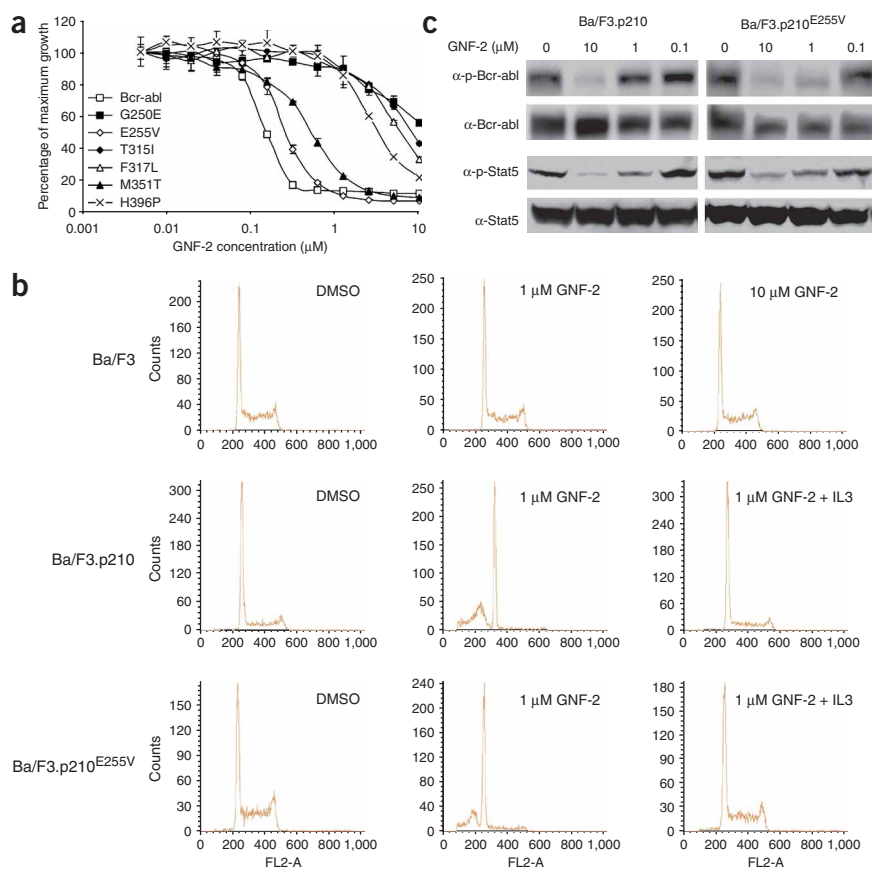


Figure 2 GNF-2 blocks proliferation and induces apoptosis of Ba/F3 cells expressing wild-type Bcr-abl and the E255V mutant. **(a)** Ba/F3 cells transformed with imatinib-resistant Bcr-abl alleles were treated with increasing concentrations of GNF-2 for 48 h. Cell viability was determined by MTT uptake and is represented as a percentage of growth in the absence of the compound. **(b)** GNF-2-induced apoptosis of wild-type or E255V mutant Bcr-abl-expressing cells is rescued by IL-3. Cells were treated for 48 h with 1 or 10 μM GNF-2 and stained with propidium iodide. The percentage of apoptotic cells was then determined by flow cytometry. Control cells were treated with DMSO. FL2-A, pulse area of propidium iodide fluorescence signal. **(c)** GNF-2 inhibits Bcr-abl-mediated cellular tyrosine phosphorylation. Ba/F3 cells expressing wild-type or E255V mutant Bcr-abl were incubated in the presence of increasing concentrations of GNF-2 (0.1, 1 and 10 μM) for 90 min. Immunoblotting of Bcr-abl and Stat5 was performed with phospho-specific antibodies to phospho-c-abl (Tyr245) and to phospho-Stat5 (Tyr694) (α-p-Bcr-abl and α-p-Stat5, respectively), or with antibodies to abl and to Stat5 (α-Bcr-abl and α-Stat5, respectively).

on Ba/F3.p210 and Ba/F3.p210^{E255V} cells was totally reversed (**Fig. 2b**) and cell viability was unaffected by up to 10 μM GNF-2 (data not shown). Cells treated with DMSO (0.1%) remained viable throughout the experiment.

GNF-2 inhibits Bcr-abl and Stat5 tyrosine phosphorylation

To determine whether the antiproliferative activity of GNF-2 was accompanied by inhibition of cellular Bcr-abl tyrosine kinase activity, Ba/F3.p210 and Ba/F3.p210^{E255V} cells were cultured in the presence of increasing concentrations of GNF-2. Cellular proteins were extracted after a 90-min treatment period and analyzed for phosphotyrosine content. The inhibition of total cellular Bcr-abl tyrosine phosphorylation was first determined using wild-type Bcr-abl-expressing cells by a capture enzyme-linked immunosorbent assay (ELISA). GNF-2 inhibited the cellular tyrosine phosphorylation of Bcr-abl in a dose-dependent manner with an IC₅₀ of 267 nM. In the same assay, imatinib inhibited Bcr-abl cellular tyrosine phosphorylation with an IC₅₀ value of 204 nM.

The concentrations of GNF-2 required to inhibit Bcr-abl autophosphorylation were determined by measuring Y245 phosphorylation by immunoblotting. At 90 min, autophosphorylation levels started to decrease at a concentration of 1 μM and were barely detectable at 10 μM, whereas the level of total Bcr-abl remained unchanged (**Fig. 2c**). Treatment of Ba/F3.p210 cells with GNF-2 induced a significant decrease in the levels of phospho-Stat5 (signal transducer and activator of transcription 5; Y694) that was detectable at 1 μM. Similar treatment of Ba/F3.p210^{E255V} cells for 90 min inhibited Bcr-abl-mediated tyrosine phosphorylation (**Fig. 2c**). Phosphotyrosine levels remained unaffected after treatment of mutant G250E, T315I and M351T Bcr-abl-expressing cells with 10 μM GNF-2 (data not shown), in accordance with the lack of antiproliferative effect on those cells.

GNF-2 does not inhibit NPM-abl- or Tel-abl-dependent proliferation

To investigate whether the ability of GNF-2 to block Bcr-abl-dependent proliferation required the Bcr, SH3 and SH2 domains, we tested whether GNF-2 could inhibit the proliferation of Ba/F3 cells transformed with different nucleophosmin (NPM) or translocation ets leukemia (Tel) fusion constructs (**Fig. 3a**). The NPM-abl fusion construct consists of 117 amino acids corresponding to the NPM oligomerization domain directly fused to the abl kinase domain, thus lacking the SH3 and SH2 abl domains. The Tel-abl constructs consist of the dimerization domain of Tel transcription factor fused upstream of the SH3 or SH2 domains of human c-abl (Ba/F3.Tel-SH3-SH2-KD and Ba/F3.Tel-SH2-KD). GNF-2 did not inhibit Ba/F3.NPM-abl, Ba/F3.Tel-SH3-SH2-KD and Ba/F3.Tel-SH2-KD cell proliferation at concentrations below 5–10 μM. In contrast,

imatinib inhibited the proliferation of NPM-abl-, Tel-SH3-SH2-KD- and Tel-SH2-KD Ba/F3-expressing cells with IC₅₀ values of 393, 88 and 55 nM, respectively. These results indicate that the abl kinase domain is not sufficient for GNF-2 to inhibit Bcr-abl-dependent cell proliferation and that it requires Bcr and/or the abl SH3 and/or the SH2 domains to do so.

GNF-2 does not inhibit c-abl kinase activity *in vitro*

To correlate the cellular inhibition of Bcr-abl with the *in vitro* inhibition of abl kinase activity, we first carried out radioenzymatic assays on the abl catalytic domain and on a construct that contained the SH3-SH2 and abl catalytic domains. GNF-2 did not inhibit phosphorylation of an exogenous abl peptide substrate (data not shown) or abl autophosphorylation at concentrations up to 10 μM (**Fig. 3b**). *In vitro* inhibition of full-length wild-type Bcr-abl was also evaluated by measuring the autophosphorylation of immunoprecipitated Bcr-abl (**Fig. 3c**). The results were similar to those obtained with

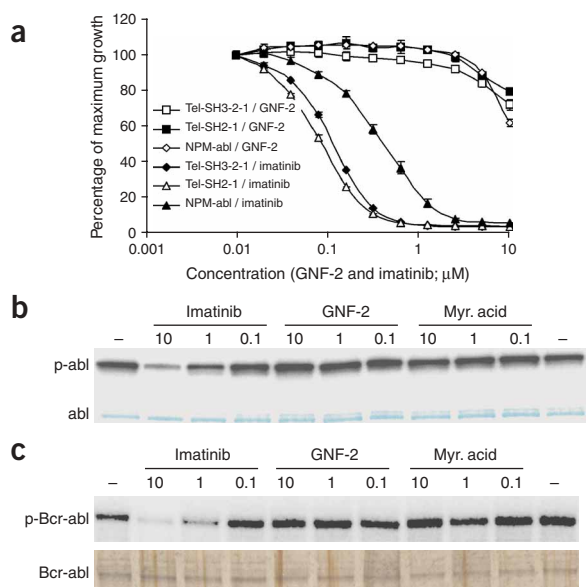


Figure 3 Construct-dependent inhibition of abl activity by GNF-2. (a) GNF-2 does not affect viability of NPM-abl-, Tel-SH3-SH2-KD abl (Tel-SH3-2-1)- and Tel-SH2-KD abl (Tel-SH2-1)-transformed Ba/F3 cells. Cells were incubated in the presence of increasing concentrations (0.010–10 μ M) of GNF-2 or imatinib for 48 h. Cell viability at 48 h was measured by MTT uptake. Each point is the mean of duplicate experiments and indicates growth expressed as a percentage of cell growth in the absence of compound. (b,c) GNF-2 does not inhibit abl kinase activity *in vitro*. *In vitro* radioenzymatic kinase assays were performed with recombinant abl (SH3-SH2-kinase domains; Coomassie stained) or immunoprecipitated Bcr-abl (silver stained) in the presence of GNF-2, imatinib or myristic (Myr.) acid. Autoradiograms show the extent of autophosphorylation of either abl (b) or Bcr-abl (c).

the catalytic domain and confirmed the lack of inhibitory activity of GNF-2 on abl kinase in cell-free systems.

GNF-2 does not inhibit *in vitro* activity of a panel of kinases

To determine whether GNF-2 could inhibit other kinases, it was tested at a concentration of 10 μ M against a panel (Upstate KinaseProfiler) of 63 kinases. The kinase panel included serine and threonine (CDK1, c-Raf-1, PDK1, PKA, PKB), and receptor (FGFR-1/3, Flt-1/3/4, HER-1/2, IGF-1R, IR, KDR, c-kit, c-Met, PDGFR β , Tie-2) and nonreceptor (Bmx, BTK, Lck, c-Src) tyrosine kinases. None of the tested kinases was significantly inhibited by 10 μ M GNF-2 (Supplementary Table 2 online).

GNF-2 binds to abl

Even though GNF-2 did not inhibit the *in vitro* kinase activity of either the abl catalytic domain or the SH3-SH2-catalytic domains, we sought

to determine whether GNF-2 could directly interact with abl. We addressed this question by immobilizing the compound onto Sepharose beads through a benzamide polyethylene glycol linker (Fig. 4a). A negative control matrix was prepared by methylation of the aniline nitrogen at the 4 position of the pyrimidine, which is a substitution that the cellular structure-activity relationships had previously demonstrated abolished activity. To verify that linker modification did not abrogate the antiproliferative effect against Bcr-abl-transformed cells, GNF-3 (3) and GNF-4 (4) were tested in proliferation assays. Although the potency of GNF-3 against Ba/F3.p210 was approximately ten-fold lower than that of GNF-2, it still maintained differential cytotoxicity as compared with Ba/F3 cells. The negative control compound (GNF-4) was devoid of antiproliferative activity on Ba/F3.p210 or Ba/F3 cells at concentrations up to 10 μ M.

The immobilized compounds were incubated with both conformationally active (Src phosphorylated) and unphosphorylated (tyrosine phosphatase-treated)¹ recombinant human abl (SH2-kinase domains), and after extensive washes the bound protein was detected by immunoblotting. The 4,6-disubstituted pyrimidine (GNF-3) bound abl independently of its activation state, whereas there was no detectable binding to the methylated compound (GNF-4) (Fig. 4b). To determine whether GNF-2 could bind to Bcr-abl from a complex protein mixture, we performed affinity chromatography experiments using Ba/F3.p210 cell extracts. Sepharose-immobilized GNF-2 bound to a 210-kDa protein identified as Bcr-abl by western

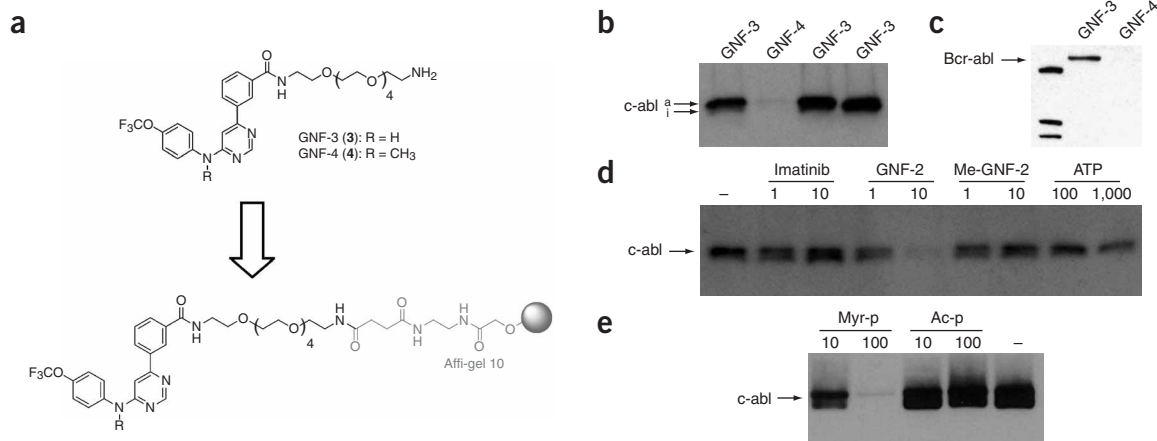


Figure 4 GNF-2 binds recombinant abl and Bcr-abl. (a) Chemical structures of GNF-3 (3), its methylated analog GNF-4 (4) and the corresponding affinity matrices. (b) Sepharose-immobilized GNF-3 was incubated with dephosphorylated (i-abl) or fully phosphorylated recombinant (a-abl) abl. After extensive washing, the bound protein was resolved by SDS-PAGE and immunodetected with anti-abl. Immobilized GNF-4 was used as a control resin. (c) Sepharose-immobilized GNF-3 was incubated with Ba/F3.p210 protein extract. After extensive washing, the bound proteins were resolved by SDS-PAGE and immunoblotted with anti-abl. (d,e) Competition experiments were performed by adding 1 or 10 μ M of imatinib, GNF-2, methyl-GNF-2 (Me-GNF-2), 0.1 or 1 mM ATP, and 10 or 100 μ M Myr-GQQPGKVLGDQRRPSL (Myr-p) or Ac-GQQPGKVLGDQRRPSL (Ac-p) peptides.

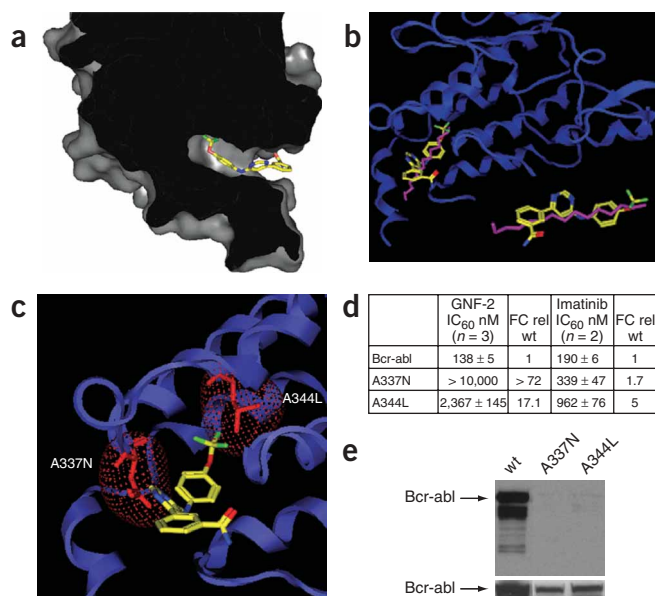


Figure 5 Model of GNF-2 bound to the abl crystal structure (PDB entry 1OPK). **(a)** GNF-2 docked in the abl myristoyl binding pocket. A cutaway rendition of the molecular surface of abl is shown. **(b)** Superimposition of myristoyl from crystal structure (PDB entry 1OPK) and docked GNF-2. The C-terminal α helices comprising the myristoyl binding pocket are shown in the ribbon diagram. Bottom right: a close-up superimposition of myristoyl and GNF-2. **(c)** Model showing mutations within the abl myristoyl pocket affecting GNF-2 activity. Mutations A337N and A344L are depicted in red in the c-abl ribbon. Molecular surfaces of A337N and A344L are shown in red dots, and GNF-2 overlaps with the A337N and A344L surface. **(d)** Antiproliferative effect of GNF-2 on A337N and A344L Bcr-abl mutants. GNF-2 antiproliferative IC₅₀ values (nM) against Ba/F3.p210, Ba/F3.p210^{A337N} and Ba/F3.p210^{A344L} cells are shown as the average of duplicate or triplicate experiments \pm s.d. Fold changes (FC) in IC₅₀ are calculated with respect to that on Ba/F3.p210 cells. **(e)** Sepharose-immobilized GNF-3 was incubated with Ba/F3.p210, Ba/F3.p210^{A337N} and Ba/F3.p210^{A344L} protein extract in the presence of 10 mM ATP. After extensive washing, the bound proteins were resolved by SDS-PAGE and immunoblotted with anti-abl. Bcr-abl expression levels were determined by immunoblot on 50 μ g of total lysates (bottom). wt, wild type.

blotting with an antibody to abl, whereas no Bcr-abl was detected binding to the control matrix (Fig. 4c).

To assess the binding specificity, we performed affinity chromatography in the presence of imatinib, ATP, GNF-2 and its methyl analog. Clear competition was only observed in the presence of 10 μ M GNF-2 (Fig. 4d). Abl was not displaced from the GNF-2 resin by the methylated compound, in accordance with the lack of binding to the methylated resin. In addition, neither imatinib (up to 10 μ M) nor ATP (up to 1,000 μ M) interfered with the ability of abl to bind to the immobilized pyrimidine, indicating that the compound might bind outside the ATP binding pocket.

To investigate whether GNF-2 might be binding to the myristic binding pocket, we performed similar competition experiments using 10 and 100 μ M of either myristic acid or a N-myristoylated peptide corresponding to the N-terminal amino acids 2–16 of c-abl 1b (ref. 8). Although, in our experimental conditions, we did not observe competition with myristate up to 100 μ M (data not shown), the myristoylated peptide clearly competed with GNF-2 for binding to c-abl at 10 μ M. As a negative control, we used the same peptide with an N-terminal acetamide replacing the myristoyl group and no competition was observed at concentrations of 10 and 100 μ M (Fig. 4e).

Mutations in the myristoyl cleft confer resistance to GNF-2

Molecular docking studies to c-abl (PDB entry 1OPK (ref. 8)) gave consistently high-score solutions for GNF-2 bound to the myristoyl pocket located in the C lobe of the kinase (Fig. 5a). The docking solutions suggested that the 4,6-disubstituted pyrimidine could adopt a conformation that would overlay well with the extended alkyl chain of myristate (Fig. 5b).

To investigate whether introducing mutations to the myristoyl pocket could prevent GNF-2 from binding to Bcr-abl, we mutated two different residues within the myristoyl cleft: A337N, located at the entry and shown to activate the kinase²³, and A344L, located at the back of the cleft (Fig. 5c). GNF-2 and imatinib were tested for their ability to block the proliferation of Ba/F3 cells transformed with these mutant alleles. Both mutations resulted in significant resistance to GNF-2 while having little impact on the activity of imatinib (Fig. 5d).

To determine the effect that mutations in the myristoyl binding pocket had on Bcr-abl binding to GNF2 resin, we also performed affinity chromatography experiments using protein lysates of Ba/F3 cells expressing wild-type, A337N or A344L mutant Bcr-abl in the presence of 10 mM ATP. Both myristoyl pocket mutations appeared to be able to disrupt Bcr-abl binding to the GNF-2 resin (Fig. 5e), demonstrating that the impaired binding observed in the affinity experiments correlated with the lack of sensitivity to cellular inhibition.

GNF-2 enhances imatinib activity on Bcr-abl-expressing cells

To test whether GNF-2 could potentiate the antiproliferative activity of imatinib on Bcr-abl-expressing cells, Ba/F3.p210 cells were treated with imatinib, GNF-2 or both at concentrations that produced only a partial inhibitory effect. We showed that the combination of imatinib and GNF2 was more effective in inhibiting Ba/F3.p210 cell growth than was either inhibitor alone (data not shown). For example, when cells were treated with concentrations of imatinib and GNF-2 that did not effect cell viability alone (230 and 100 nM, respectively), the combination resulted in the survival of only 25.5 \pm 3.5% of the cells. The combination index, calculated according to the method of Chou and Talalay²⁴ using CalcuSyn software, for the imatinib–GNF-2 combination was 0.78, confirming the existence of moderate synergy between the two compounds.

DISCUSSION

Owing to the incidence of resistance to imatinib in advanced CML, many efforts are underway to find new pharmacological agents that address this challenge. Compounds of the well-known pyridopyrimidine class, such as PD180970, have recently been shown to have potent activity on a subset of mutant Bcr-abl kinases²⁵. There are now two compounds with a wide mutant activity spectrum, BMS-354825 (ref. 6) and AMN107 (ref. 5), in clinical trials for the treatment of CML patients refractory to imatinib. These compounds bind to the ATP site, thereby inhibiting abl kinase activity, which ultimately leads to the induction of apoptosis in Bcr-abl-expressing cells.

Screens for abl or other kinase inhibitors are usually performed on recombinant catalytic kinase domains at low ATP concentrations, explaining the fact that most known abl kinase inhibitors are ATP competitors. In addition, repetitive screens on recombinant catalytic domains often result in the re-identification of well-explored classes of kinase inhibitors. To circumvent this problem and to search for new mechanisms of inhibition, we performed a differential cytotoxicity screen on cells specifically transformed with Bcr-abl as compared with their isogenetic parental cell line. We identified a class of 4,6-disubstituted pyrimidine compounds, represented by GNF-1 and

GNF-2, that, despite a lack of *in vitro* inhibition of abl kinase activity, showed the same effects on Ba/F3.p210 cells as are observed for inhibitors of the imatinib type, namely inhibition of proliferation, induction of apoptosis and inhibition of Bcr-abl autophosphorylation and phosphorylation of downstream substrates (Stat5).

The characteristic that first attracted our interest in this class of compounds was the complete lack of toxicity (at concentrations up to 40 μM) toward cells not expressing Bcr-abl. This remarkable selectivity was not exclusive for cells engineered to express Bcr-abl (Ba/F3.p210 and 32D.p210), but also extended to other cell lines (K562 and SUP-B15) derived from patients with Philadelphia chromosome-positive disorders. The antiproliferative activity of GNF-2 was accompanied by an inhibition of cellular Bcr-abl tyrosine phosphorylation, with an IC_{50} value of 267 nM, and the apoptotic cell death of Bcr-abl positive cells. In addition, the antiproliferative activity of GNF-2 did not interfere with the IL-3-induced survival pathway as the compound was unable to induce Ba/F3.p210 cell death in the presence of IL-3. However, when *in vitro* kinase assays were performed on recombinant abl kinase domain, GNF-2 did not inhibit kinase activity. To investigate whether the involvement of other domains of abl kinase was critical for the activity of this class of compound, we carried out the same kinase assays using constructs that contained SH3-SH2-catalytic domains, full-length recombinant abl or immunoprecipitated Bcr-abl, measuring the extent of autophosphorylation or phosphorylation of a peptide substrate and the physiological Bcr-abl substrate CrkL (data not shown). In all cases, there was no detectable abl tyrosine kinase inhibitory activity at concentrations below 10 μM , in contrast to what would be expected for an ATP site-directed inhibitor. The excellent cellular selectivity, together with the inability of this compound to inhibit any of the 63 kinases tested in biochemical assays, including c-abl, prompted us to hypothesize that GNF-2 inhibited cellular Bcr-abl kinase activity through an allosteric non-ATP competitive mechanism of action or through an alternative cellular target. Although several allosteric kinase inhibitors have been reported, they all inhibit the *in vitro* kinase activity of their target. Examples include the pleckstrin domain-dependent Akt inhibitor Akt-I-1 (ref. 16) and the I κ B kinase (IKK) inhibitor BMS-345541 (ref. 26).

Structural and biochemical studies have shown that imatinib is not a purely ATP-competitive inhibitor; its binding extends to an adjacent hydrophobic pocket that is accessible when the activation loop adopts a conformation that renders the kinase inactive. As a consequence of its binding characteristics, not only mutations affecting the direct contact residues for the drug (for example, Thr315 and Phe317), but also mutations located in regions that affect the kinase conformation (for example, Gly250, Glu255 and Met351), are responsible for conferring resistance to imatinib. Similarly to imatinib, neither GNF-2 nor any compound of this series showed any antiproliferative effect on cells expressing G250E, Q252H, T315I or F317L Bcr-abl mutant forms. In contrast to imatinib, GNF-2 showed a strong, IL-3-reversible antiproliferative and apoptotic effect on Ba/F3.p210^{E255V} and Ba/F3.p185^{Y253H} cells, comparable with that observed on wild-type Bcr-abl-expressing cells. Despite the lack of *in vitro* Bcr-abl kinase inhibition, the cellular inhibition of Bcr-abl phosphorylation by GNF-2, together with the fact that single mutations on the abl kinase domain completely abolished GNF-2 antiproliferative activity, pointed toward the direct binding of the compound to Bcr-abl. Indeed, immobilization of the compound and affinity chromatography and competition experiments with an SH2-kinase domain abl construct demonstrated that GNF-2 specifically bound to abl. However, as the binding to the kinase seems not to be enough to inhibit *in vitro* abl catalytic activity, it is likely that a unique cellular conformation or

cofactors are required to achieve cellular activity. The requirement of a particular abl conformation for GNF-2 activity was emphasized by the fact that mutations within the P loop or activation loop, which can impair conformational changes in abl, greatly diminished the antiproliferative activity of GNF-2.

Recent investigations have shown the complexity of the regulatory mechanisms of c-abl and have provided a molecular model that can be used to explain the deregulatory role of the fusion of Bcr to abl. Crystal structures of c-abl kinase bound to a myristoylated peptide that corresponds to the N terminus of c-abl or myristic acid have been recently described⁸. The structural analysis revealed a hydrophobic pocket in the C lobe of the kinase that could accommodate the myristate attached to the N terminus of human abl 1b, stabilizing the inactive conformation of the protein. Bcr-abl is not myristoylated and lacks this autoinhibitory mechanism, but it could be expected that compounds that bind to the myristate pocket can mimic the myristoyl group and induce the inactive conformation of the kinase. Although we did not detect *in vitro* abl kinase inhibition by both GNF-2 and myristic acid at concentrations up to 10 μM (Fig. 3b), docking experiments with GNF-2 to c-abl 46-534 (PDB entry 1OPK) showed that the compound could assume an extended conformation that superimposed well on the myristate in the myristoyl binding pocket (Fig. 5b). Furthermore, introduction of mutations within the Bcr-abl myristoyl binding site had a large impact on GNF-2 cellular activity. GNF-2 antiproliferative activity was either lost ($\text{IC}_{50} > 10 \mu\text{M}$) or significantly diminished ($\text{IC}_{50} = 2,367 \text{ nM}$) by blocking the entry into the myristoyl pocket (A337N) or decreasing its depth (A344L), respectively. The substitution A337N was previously described as increasing the activity of full-length c-abl²³, presumably by blocking the entry of the myristoyl group into its pocket. As expected, imatinib's antiproliferative activity was not affected by the substitution A337N, whereas the A344L substitution resulted in a five-fold increased resistance. Consistent with these results, both mutations impaired Bcr-abl binding to immobilized GNF-2 (Fig. 5e). As is true for imatinib²⁷, the locations of the resistance-inducing mutations cannot be used alone to pinpoint the inhibitor binding site, as mutations that are proximal to the proposed binding site in the myristate pocket (A337N, A344L) and distant (T315I) both cause resistance. These results probably reflect the plasticity of protein kinases²⁸ and the ability of a mutation to exert conformational influences at a distance.

All our experimental data, together with the currently proposed mechanistic model of c-abl regulation, lead us to hypothesize that GNF-2 may stabilize the inactive conformation of Bcr-abl upon binding to the myristoyl pocket. This is consistent with the ability of a myristoylated peptide corresponding to the N terminus of c-abl to compete for the binding of GNF-2 to abl (Fig. 4e). GNF-2 binding might induce the bending of the kinase domain α -I helix (which is extended and clashes with the SH2 domain when the myristoyl pocket is not occupied^{8,23}) toward the C lobe, allowing the SH2 domain to dock to the C lobe. Subsequently, the SH3 domain can dock to the N lobe, holding the kinase in an inactive state. This hypothesis is in agreement with the ability of GNF-2 to bind to the abl SH2-kinase domain construct (Fig. 4b) and explains the inability of GNF-2 to inhibit the cellular kinase activity of NPM-abl, lacking the SH2 and SH3 domains (Fig. 3a). The lack of antiproliferative activity of GNF-2 on Ba/F3 cells expressing Tel-SH3-SH2-KD and Ba/F3.Tel-SH2-KD may be due to the ability of the Tel domain to disrupt the conformational changes or binding of other cellular cofactors required for GNF-2 activity upon binding to the myristoyl pocket. The effect of Tel on the overall conformation of the fusion proteins seems clear, as

both cell lines are more sensitive to imatinib (88 and 55 nM) than are cells expressing Bcr-abl (190 nM). This is consistent with previous reports that inhibitory activity of imatinib can be increased through the introduction of SH2-domain-binding phosphopeptides, which relieve the inhibitory constraints imposed by the SH3 and SH2 domains on abl²³.

Binding to an allosteric binding site distant from the active site of the kinase, such as the myristoyl binding cleft, would also be consistent with the exceptional cellular and enzymatic selectivity observed for this class of compounds. In contrast to imatinib, which also inhibits c-kit, PDGFR α , and PDGFR β kinases²⁹, GNF-2 does not affect the proliferation driven by any of these or by other oncogenic kinases tested. Moreover, the synergistic antiproliferative effect observed when combining GNF-2 and imatinib further supports the hypothesis that GNF-2 and imatinib bind to different Bcr-abl sites. GNF-2 binding to the myristoyl pocket of Bcr-abl could favor imatinib binding by stabilizing the inactive conformation of the enzyme, thus explaining the synergistic effect of the imatinib–GNF-2 combination. Synergistic combinations of imatinib with several non-abl inhibitors have been previously reported^{30–32}, but so far only ON012380, which presumably binds to the substrate-binding site of Bcr-abl³³, and GNF-2 are thought to exert their synergistic activity with imatinib by binding to two different sites of Bcr-abl. Further validation of the hypothesis that GNF-2 binds to the myristoyl pocket awaits structural evidence of GNF-2 binding to abl obtained through crystallography or NMR spectroscopy.

The newly described mechanism of Bcr-abl inhibition by GNF-2 and analogs, together with their exceptionally high degree of cellular and enzymatic specificity, their activity against abl resistant mutants, such as E255V (frequently found as a cause of relapse during imatinib treatment in the clinic and associated with a poor prognosis³⁴), their simple molecular structure and their good pharmacokinetic behavior in rodents, makes this class of compounds interesting candidates as the starting point for new drug development. Moreover, this class might represent the first class of leukemia-specific agents with no off-target activity; they might have safety profiles superior to those of existing agents and serve as exceptionally selective research 'tool' compounds for investigating abl-dependent phenomena.

METHODS

Cell culture. The IL-3-dependent murine pro-B cell line Ba/F3, and murine myeloid precursor cell line 32D, were maintained in RPMI-1640 medium supplemented with L-glutamine, 10% FBS and 10 U ml⁻¹ recombinant murine IL-3 (Roche). The Mo7e human megakaryoblastic cell line was grown in RPMI-1640 medium supplemented with L-glutamine, 20% FBS and 5 ng ml⁻¹ recombinant human granulocyte-macrophage colony stimulating factor (R&D Systems) or 200 ng ml⁻¹ stem cell factor (Biosource).

Wild-type Bcr-abl-expressing 32D (32D.p210) and Ba/F3 (Ba/F3.p210) cells, and mutant Bcr-abl-expressing cell lines Ba/F3.p210^{G250E}, Ba/F3.p210^{E255V}, Ba/F3.p210^{T315I}, Ba/F3.p210^{F317L} and Ba/F3.p210^{M351T}, as well as Ba/F3 cells transformed with Flt-3-ITD kinase were obtained from J.D. Griffin (Dana Farber Cancer Institute, Boston). Ba/F3 cells expressing the fusion protein kinases Tel-PDGFR β and Tel-JAK1 were obtained from G. Gilliland (Harvard Medical School, Boston), and Ba/F3.TPR-MET cells were acquired from R. Salgia (Pritzker School of Medicine, University of Chicago). All the above cell lines were maintained in RPMI-1640 medium with L-glutamine, 10% FBS and 1 mg ml⁻¹ geneticin (Gibco).

Ba/F3.p185^{Q252H}, Ba/F3.p185^{Y253H} and Ba/F3 cells expressing the fusion protein kinase NPM-abl were provided by J. Duyster (Technical University of Munich) and maintained in RPMI-1640 medium with L-glutamine and 10% FBS.

Human leukemic cell lines K562 (p210 Bcr-abl-expressing chronic myelogenous leukemia), HL-60 (acute promyelocytic leukemia), SUP/B15 (p190

Bcr-abl-expressing acute lymphoblastic leukemia) and Jurkat (acute T cell leukemia) were purchased from the American Type Culture Collection and cultured following their recommendations.

Proliferation assays. Cells ($0.3\text{--}0.6 \times 10^6$ per ml) were plated in duplicate or triplicate in 96-well plates containing increasing drug concentrations (0.005–10 μM). After incubation at 37 °C in 5% CO₂ for 48 h, the effect of the compounds on cell viability was determined by the MTT (3-(4,5-dimethylthiazolyl-2)-2,5-diphenyltetrazolium bromide; Promega) colorimetric dye reduction method. Inhibition of cell proliferation was calculated as a percentage of growth of DMSO-treated cells, and IC₅₀ values were determined with Microsoft Excel XLfit3.

Simultaneous treatment of Ba/F3.p210 cells with imatinib and GNF-2 was carried out to evaluate the synergistic or additive effect of the drug combinations on cellular proliferation. Cells treated with increasing concentrations of each compound alone or in combination were incubated at 37 °C in 5% CO₂ for 48 h, and cell viability was determined by the MTT assay. The *in vitro* additive, synergistic or antagonistic effect was determined by calculating the combination index from two independent experiments using CalcuSyn Software (Biosoft).

Phosphotyrosine analysis. The total cellular tyrosine phosphorylation levels of Bcr-abl were first determined using capture ELISA. Bcr-abl-expressing cells treated for 90 min with various concentrations of test compound were homogenized in lysis buffer (50 mM Tris-HCl pH 7.4, 150 mM NaCl, 5 mM EDTA, 1 mM EGTA, 1% Nonidet P-40, 2 mM Na₂VO₄ and protease inhibitor cocktail (Roche)); the lysates were then plated on 96-well plates containing adsorbed polyclonal antibody to Abl SH3 domain (Upstate Biotechnology). The plates were incubated for 4 h at 4 °C and then washed with PBS/0.05% Tween 20 buffer. To detect phosphotyrosine residues, alkaline phosphatase-conjugated monoclonal antibody to phosphotyrosine (PY20; Zymed Laboratories) was added to each well, and plates were incubated overnight at 4 °C. The wells were then washed with PBS/0.05% Tween 20 buffer, and 100 μl per well of CDP-Star Substrate with Emerald-II enhancer substrate (Applied Biosystems) was added. After 45 min, light emission was quantified with a GeminiXS microplate reader (Molecular Devices). Bcr-abl phosphotyrosine content was calculated as a percentage of phosphotyrosine of untreated cells, and IC₅₀ values were determined with Microsoft Excel XLfit3.

The state of tyrosine phosphorylation of cellular Bcr-abl and its substrate Stat5 after drug treatment was determined by western blotting with phospho-specific antibodies. Ba/F3.p210 and Ba/F3.p210^{E255V} cells were incubated in the presence of various concentrations of GNF-2 and, after 1.5 h incubation, lysed in lysis buffer (20 mM Tris-HCl (pH 7.5), 150 mM NaCl, 1 mM Na₂EDTA, 1 mM EGTA, 1% Triton, 2.5 mM sodium pyrophosphate, 1 mM β -glycerophosphate, 1 mM Na₂VO₄, 1 $\mu\text{g ml}^{-1}$ leupeptin, 1 mM PMSF). Equal amount of lysate (50 μg) were subjected to SDS-PAGE followed by immunoblotting with phospho-specific antibodies—anti-phospho-c-abl (Tyr245), and anti-phospho-Stat5 (Tyr694) (Cell signaling) antibodies—or antibodies recognizing Bcr-abl (Ab-3; Oncogene Science) and Stat5 (C-17; Santa Cruz Biotechnology). Proteins were detected by enhanced chemiluminescence (ECL-plus; Amersham), following manufacturer's guidelines.

Kinase assays. *In vitro* kinase assays were carried out using recombinant c-abl containing SH3, SH2 and kinase domains (residues 46–531) and full-length immunoprecipitated Bcr-abl. Recombinant abl was expressed in Sf9 insect cells and purified as described in the **Supplementary Methods** online. Bcr-abl immune complexes were obtained with Ab-3 monoclonal antibody to abl (Oncogene Science) from Ba/F3.p210 lysates as described³⁵.

Volumes of 1 μg of recombinant abl or immunoprecipitated Bcr-abl (from 3×10^6 cells) were incubated with various concentrations of test compound (0.1, 1, 10 μM) in kinase buffer (50 mM Tris-HCl pH 7.5, 10 mM MgCl₂, 100 μM EDTA, 1 mM DTT, 0.015% Brij 35), 100 μM ATP and 1 μCi [γ -³²P]ATP for 30 min at 30 °C. The reaction was stopped by addition of Laemmli buffer (Bio-Rad Laboratories), and the proteins were resolved by SDS-PAGE in a 4–20% gel. The phosphoproteins were visualized by autoradiography and the autophosphorylation quantified using a phosphoimager (STORM; Molecular Devices).

Affinity chromatography with immobilized compounds. Bcr-abl-expressing Ba/F3 cells were harvested and lysed as described. Total cellular proteins (0.5 mg) or recombinant c-abl (1 µg) were mixed with 100 µl of 50% suspension of immobilized GNF-3 or with a 50% suspension of immobilized methyl-GNF3 (GNF-4). The samples were incubated for 1 h at 4 °C on a rotation mixer. After incubation, the resin was washed five times with buffer (50 mM Tris pH 7.4, 250 mM NaCl, 5 mM EDTA, 5 mM EGTA, 5 mM NaF, 0.1% Nonidet P-40 and protease inhibitors (Sigma)) and suspended in 50 µl of Laemmli buffer. After heat denaturation at 95 °C for 5 min, the bound proteins were resolved by SDS-PAGE and identified by western blotting.

Note: Supplementary information is available on the Nature Chemical Biology website.

ACKNOWLEDGMENTS

We thank J.D. Griffin, G. Gilliland, R. Salgia and J. Duyster for kindly providing us with cell lines, and C. Trussell, D. Kemp, M. Warmuth and S. Kim for their help and valuable discussions.

COMPETING INTERESTS STATEMENT

The authors declare that they have no competing financial interests.

Published online at <http://www.nature.com/naturechemicalbiology/>
Reprints and permissions information is available online at <http://npg.nature.com/reprintsandpermissions/>

1. Schindler, T. *et al.* Structural mechanism for STI-571 inhibition of Abelson tyrosine kinase. *Science* **289**, 1938–1942 (2000).
2. Gorre, M.E. *et al.* Clinical resistance to STI-571 cancer therapy caused by BCR-ABL gene mutation or amplification. *Science* **293**, 876–880 (2001).
3. von Bubnoff, N., Schneller, F., Peschel, C. & Duyster, J. BCR-ABL gene mutations in relation to clinical resistance of Philadelphia-chromosome-positive leukaemia to STI571: a prospective study. *Lancet* **359**, 487–491 (2002).
4. Cowan-Jacob, S.W. *et al.* Imatinib (STI571) resistance in chronic myelogenous leukemia: molecular basis of the underlying mechanisms and potential strategies for treatment. *Mini Rev. Med. Chem.* **4**, 285–299 (2004).
5. Weisberg, E. *et al.* Characterization of AMN107, a selective inhibitor of native and mutant Bcr-Abl. *Cancer Cell* **7**, 129–141 (2005).
6. Shah, N.P. *et al.* Overriding imatinib resistance with a novel ABL kinase inhibitor. *Science* **305**, 399–401 (2004).
7. Superti-Furga, G. & Courtneidge, S.A. Structure-function relationships in Src family and related protein tyrosine kinases. *Bioessays* **17**, 321–330 (1995).
8. Nagar, B. *et al.* Structural basis for the autoinhibition of c-Abl tyrosine kinase. *Cell* **112**, 859–871 (2003).
9. Barker, A.J. *et al.* Studies leading to the identification of ZD1839 (IRESSA): an orally active, selective epidermal growth factor receptor tyrosine kinase inhibitor targeted to the treatment of cancer. *Bioorg. Med. Chem. Lett.* **11**, 1911–1914 (2001).
10. Meijer, L. *et al.* Biochemical and cellular effects of roscovitine, a potent and selective inhibitor of the cyclin-dependent kinases cdc2, cdk2 and cdk5. *Eur. J. Biochem.* **243**, 527–536 (1997).
11. Buchdunger, E. *et al.* Inhibition of the Abl protein-tyrosine kinase in vitro and in vivo by a 2-phenylaminopyrimidine derivative. *Cancer Res.* **56**, 100–104 (1996).
12. Regan, J. *et al.* Pyrazole urea-based inhibitors of p38 MAP kinase: from lead compound to clinical candidate. *J. Med. Chem.* **45**, 2994–3008 (2002).
13. Lyons, J.F., Wilhelm, S., Hibner, B. & Bollag, G. Discovery of a novel Raf kinase inhibitor. *Endocr. Relat. Cancer* **8**, 219–225 (2001).
14. Lowinger, T.B., Riedl, B., Dumas, J. & Smith, R.A. Design and discovery of small molecules targeting raf-1 kinase. *Curr. Pharm. Des.* **8**, 2269–2278 (2002).
15. Ohren, J.F. *et al.* Structures of human MAP kinase kinase 1 (MEK1) and MEK2 describe novel noncompetitive kinase inhibition. *Nat. Struct. Mol. Biol.* **11**, 1192–1197 (2004).
16. Barnett, S.F. *et al.* Identification and characterization of pleckstrin-homology-domain-dependent and isoenzyme-specific Akt inhibitors. *Biochem. J.* **385**, 399–408 (2005).
17. Grimsby, J. *et al.* Allosteric activators of glucokinase: potential role in diabetes therapy. *Science* **301**, 370–373 (2003).
18. Ding, S., Gray, N.S., Wu, X., Ding, Q. & Schultz, P.G. A combinatorial scaffold approach toward kinase-directed heterocycle libraries. *J. Am. Chem. Soc.* **124**, 1594–1596 (2002).
19. Goldman, J.M. & Melo, J.V. Chronic myeloid leukemia—advances in biology and new approaches to treatment. *N. Engl. J. Med.* **349**, 1451–1464 (2003).
20. Druker, B.J. *et al.* Effects of a selective inhibitor of the Abl tyrosine kinase on the growth of Bcr-Abl positive cells. *Nat. Med.* **2**, 561–566 (1996).
21. Carroll, M. *et al.* CGP 57148, a tyrosine kinase inhibitor, inhibits the growth of cells expressing BCR-ABL, TEL-ABL, and TEL-PDGFR fusion proteins. *Blood* **90**, 4947–4952 (1997).
22. Dorsey, J.F. *et al.* Interleukin-3 protects Bcr-Abl-transformed hematopoietic progenitor cells from apoptosis induced by Bcr-Abl tyrosine kinase inhibitors. *Leukemia* **16**, 1589–1595 (2002).
23. Hantschel, O. *et al.* A myristoyl/phosphotyrosine switch regulates c-Abl. *Cell* **112**, 845–857 (2003).
24. Chou, T.C. & Talalay, P. Quantitative analysis of dose-effect relationships: the combined effects of multiple drugs or enzyme inhibitors. *Adv. Enzyme Regul.* **22**, 27–55 (1984).
25. von Bubnoff, N. *et al.* Inhibition of wild-type and mutant Bcr-Abl by pyridopyrimidine-type small molecule kinase inhibitors. *Cancer Res.* **63**, 6395–6404 (2003).
26. Burke, J.R. *et al.* BMS-345541 is a highly selective inhibitor of IκB kinase that binds at an allosteric site of the enzyme and blocks NF-κB-dependent transcription in mice. *J. Biol. Chem.* **278**, 1450–1456 (2003).
27. Nardi, V., Azam, M. & Daley, G.Q. Mechanisms and implications of imatinib resistance mutations in BCR-ABL. *Curr. Opin. Hematol.* **11**, 35–43 (2004).
28. Huse, M. & Kuriyan, J. The conformational plasticity of protein kinases. *Cell* **109**, 275–282 (2002).
29. Capdeville, R., Buchdunger, E., Zimmermann, J. & Matter, A. Glivec (STI571, imatinib), a rationally developed, targeted anticancer drug. *Nat. Rev. Drug Discov.* **1**, 493–502 (2002).
30. Klejman, A., Rushen, L., Morrione, A., Slupianek, A. & Skorski, T. Phosphatidylinositol-3 kinase inhibitors enhance the anti-leukemia effect of STI571. *Oncogene* **21**, 5868–5876 (2002).
31. Sun, X., Layton, J.E., Elefanti, A. & Lieschke, G.J. Comparison of effects of the tyrosine kinase inhibitors AG957, AG490, and STI571 on BCR-ABL-expressing cells, demonstrating synergy between AG490 and STI571. *Blood* **97**, 2008–2015 (2001).
32. Topaly, J., Zeller, W.J. & Fruehauf, S. Synergistic activity of the new ABL-specific tyrosine kinase inhibitor STI571 and chemotherapeutic drugs on BCR-ABL-positive chronic myelogenous leukemia cells. *Leukemia* **15**, 342–347 (2001).
33. Gumireddy, K. *et al.* A non-ATP-competitive inhibitor of BCR-ABL overrides imatinib resistance. *Proc. Natl. Acad. Sci. USA* **102**, 1992–1997 (2005).
34. Branford, S. *et al.* Detection of BCR-ABL mutations in patients with CML treated with imatinib is virtually always accompanied by clinical resistance, and mutations in the ATP phosphate-binding loop (P-loop) are associated with a poor prognosis. *Blood* **102**, 276–283 (2003).
35. Danhauser-Riedl, S., Warmuth, M., Druker, B.J., Emmerich, B. & Hallek, M. Activation of Src kinases p53/56^{lvm} and p59^{hck} by p210^{bcr/abl} in myeloid cells. *Cancer Res.* **56**, 3589–3596 (1996).